IOP Publishing Superconductor Science and Technology
Supercond. Sci. Technol. 31 (2018) 085007 (6pp) https://doi.org/10.1088/1361-6668/aacd89

Coherent transmission of superconducting carriers through a $\sim 2\,\mu$m polar semiconductor

Himadri Chakraborti[1], Swarup Deb[1], Rüdiger Schott[2], Varun Thakur[3], Abhijit Chatterjee[3], Santosh Yadav[1], Rajendra K Saroj[1], Andreas Wieck[2], S M Shivaprasad[3], K Das Gupta[1] and S Dhar[1]

[1] Department of Physics, Indian Institute of Technology Bombay, Mumbai 400076, India
[2] Lehrstuhl für Angewandte Festkörperphysik, Ruhr Universität Bochum, D-44801 Bochum, Germany
[3] Chemistry and Physics of Materials Unit, Jawaharlal Nehru Centre for Advanced Scientific Research, Bengaluru 560064, India

E-mail: kdasgupta@phy.iitb.ac.in

Received 6 April 2018, revised 4 June 2018
Accepted for publication 19 June 2018
Published 10 July 2018

Abstract

Coherent transmission of Cooper pairs through a non-superconducting medium is a key challenge for hybrid electronics with superconductors, normal metals and semiconductors. While superconductor–normal metal–superconductor (SNS) junctions have been known for quite sometime, including a low carrier density region or a two-dimensional electron gas (2DEG) in the path of superconducting electrons is relatively less explored. Indeed, this is due to the limited choice of materials that would make ohmic contacts to such systems, while simultaneously supporting a superconducting phase. In this paper we show a coherent transmission of supercurrent through a degenerate semiconductor over a length ≈ 2 μm with a critical magnetic field $B_c \approx 8$ T at 1.6 K and $T_c \approx 5$ K at zero magnetic field. This length scale is much larger than the typical thickness of a Josephson junction. Our system is a fragment of a GaN nanowall network that has been shown to support a high mobility 2DEG ($\mu_n > 10^4\,\mathrm{cm^2\,V^{-1}\,s^{-1}}$). The current and voltage probes were superconducting tungsten–gallium composite electrodes and the measurements could be done in four-probe geometry. We demonstrate ballistic type carrier transport with a near ideal transparency of 1 and a critical current (I_c) large enough such that the Josephson coupling parameter $\hbar I_c / e k_B T_c \gg 1$. Some features in magneto-transport data suggest that there is possibly a small magnetic moment forming in the semiconductor fragment. In addition the combination of a T_c typical of elemental metallic superconductors, but a critical field that appears to be higher than the Clogston–Chandrasekhar limit, may be indicative of the emergence of a triplet pairing mechanism in these structures.

Keywords: superconductor–semiconductor interface, Josephson junction, 2D electron gas, spin-triplet

(Some figures may appear in colour only in the online journal)

Superconductor (S)–semiconductor (Sm) hybrid systems are possible hosts for new composite excitations and topological states of matter [1, 2]. They have immense potential in emerging fields like superconducting electronics [3] and quantum computation [4]. A superconductor placed in contact with a semiconductor (or any other normal conductor), may induce superconductivity in the latter by proximity [5]. Spatial extent of this effect depends on the scattering length of the carriers in the semiconductor as well as the transparency of the interface. In this context, two-dimensional electron gas (2DEG) systems are particularly interesting as they offer much higher mobility than their bulk counterparts. Longer carrier lifetimes enhance the possibility of sustaining coherent states longer. Proximity effect in high mobility 2DEG systems

such as GaAs/AlGaAs, InAs/InGaAs heterostructures as well as graphene from various superconducting materials have been reported [6–9]. However, obtaining high transparency (low probability of non-Andreev reflections) at the S–Sm junction is a challenge. In this paper we address this issue from an experimental perspective.

Recently, formation of a 2DEG was demonstrated in a wedge shaped polar semiconductor with no heterointerface [10]. If the surface is tapered along the direction of polarization, spontaneous polarization can lead to the development of charges of identical polarity on the two inclined faces forming the taper. Self-consistent calculations show that the charge separation leads to the formation of a confined high mobility channel in the central plane. This mode of 2D carrier confinement can lead to a significant enhancement of carrier mobility in wurtzite–GaN, which has a spontaneous polarization along the *c*-axis. There are several reports of growth of *c*-axis oriented wedge shaped GaN nanowall network on sapphire substrates using molecular beam epitaxy (MBE) [11–14]. The walls are typically 100–200 nm wide at the base and less than 20 nm wide at the tip. Electron mobility through these is measured to be about two orders of magnitude larger than that in GaN bulk and has very little temperature dependence [12, 15, 16]. Weak localization with a coherence length of $\approx$60 μm, has been observed at $T \sim 2$ K in these [4, 15, 16]. Quantum confinement of carriers is also supported by the blue shift of photoluminescence and photo-conductance line-shapes [17]. Non annealed but high transparency ohmic contact can be made to this channel. This leads to the possibility of injecting supercurrents, which is considerably more difficult to do in a conventional 2DEG at a heterointerface like that of GaAs and AlGaAs.

In this paper we report supercurrent flow in S–Sm–S structures made of amorphous tungsten leads connecting individual wedge shaped GaN nanowall network fragments. GaN nanowall network sample was grown directly on *c*-plane sapphire substrates using plasma assisted MBE technique at a substrate temperature of 630 °C, Ga flux of 3.86×10^{14} cm^{-2} s^{-1} and nitrogen flow rate of 4.5 sccm [11]. These were then mechanically dislodged from the host substrate and cast on a Si/SiO_2 wafer, pre-patterned with 120 μm $\times$ 120 μm contact pads Ti(20 nm)/Au(50 nm), separated by 45 μm. A few of these were then connected with the Ti/Au pads by amorphous tungsten tracks using gas-assisted focused ion beam (FIB) technique. The tungsten was carried by a hexacarbonyl tungsten ($W(CO)_6$) gas and then selectively decomposed by a gallium beam (30 keV Ga^+, 52 pA ion current) leaving an amorphous tungsten–gallium film at programmed locations forming the leads. The material behaves as a 'dirty' superconductor with a high critical field. We observed that the supercurrent flows through the semiconductor for contact separations as large as $\approx$2 μm up to a critical magnetic field $B_c \approx 8$ T at 1.6 K and $T_c \approx 5$ K at zero magnetic field. Several dummy W-strips of different widths were also drawn between Ti/Au contact pads using the same technique to investigate the superconducting property of the contact lines (device D2). The temperature dependence of the critical current shows ballistic type carrier transport through the S–Sm–S structure with a near ideal transparency of 1.

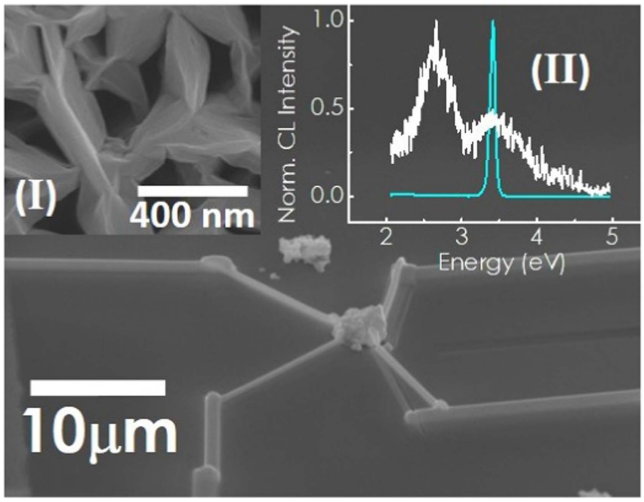

Figure 1. SEM image of device D1a. Inset (I): SEM micrograph of the wall network. Inset (II): cathodoluminescence (CL) profiles for the same fragment (broad white line) and a continuous GaN epitaxial layer (sharp blue peak). One of the two broad features in the CL response from the area where the GaN fragment is coincides with the location of the response from the epitaxial layer, the broad feature at the lower energy most likely originates from the surrounding silicon oxide and the metallic tracks laid down by the focussed ion process.

Table 1. Configuration of the devices.

Device	Contact/type	Residual R (Ω)
D1a	Three-probe W/GaN	0
D1b	Three-probe W/GaN	150
D1c	Two-probe W/GaN	300
D2	Four-probe W strip (control)	0

Measurements were carried out on four devices (see table 1). D1a had four contacts , D1b and D1c had three and two contacts respectively. The observed resistance drop in each case was consistent with the known lead resistance of the cryostat wiring (150 Ω), the residual resistance in the two-probe device D1c being twice of that of the three-probe device D1b. We also found that the two-probe resistance of the device, in its normal state, remained less than $h/4e^2 \approx 6.4\,\mathrm{k}\Omega$. The low value of the shunt resistance is also evident in the overdamped nature of the *I–V* curve of D1a.

The devices were characterized using energy dispersive x-ray spectroscopy attached with a scanning electron microscopy (SEM) as well as room temperature CL spectroscopy in order to confirm that the device material is indeed GaN.

Figure 1 shows the SEM image of D1a. Inset (I) of the figure shows the SEM surface view of the wall network from which the fragment in D1a is dislodged. Inset (II) of the figure compares the CL band-edge profiles for the same fragment and a GaN epitaxial layer grown in the same chamber. The position of the high energy feature for the fragment agrees with that of GaN film. Figure 2(a) shows the resistance of the

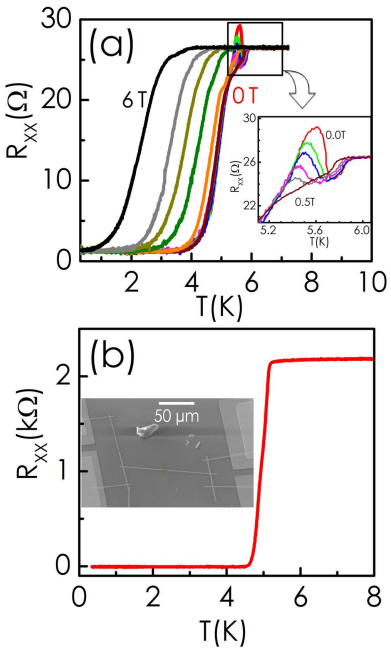

Figure 2. (a) $R(T)$ measured for device D1a at different magnetic fields ($B_\perp = 0$, 0.05, 0.1, 0.2, 0.3, 0.5, 1, 2, 3, 4, 6 T). Inset shows the evolution of anomalous resistance peak with the magnetic field. (b) Temperature variation of the resistance for device D2. Measurements were done using a four-probe a.c. lock in method with a current of ≈100 nA at 127 Hz. The inset shows an SEM micrograph of the control sample D2.

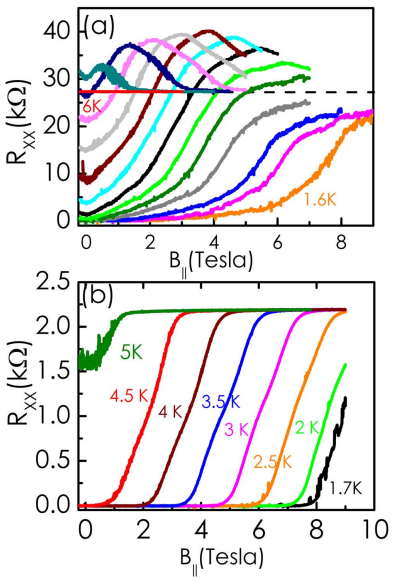

Figure 3. (a) Resistance of the wall fragment $R_{gn}(B)$ measured at different temperatures (consecutively at $T = 1.60$, 2.50, 2.75, 3.25, 3.50, 3.75, 4.00, 4.25, 4.50, 4.75, 5, 5.25, 5.50 and 6.00 K) as a function of magnetic field applied parallel to the substrate. (b) Resistance versus magnetic field (parallel to the substrate) observed for device D2.

GaN wall fragment (R_{gn}) as a function of temperature T for different magnetic fields ($B_\perp$) normal to the substrate. D1b and D1c were also found to show sharp drop in resistance below ≈5 K, consistent with superconducting transitions. Figure 2(b) shows the resistance of the tungsten strip, R_w (Device D2) measured at different magnetic fields as a function of T. R_w also shows a transition to superconductivity. Superconducting transition with $T_c \approx 5$ K has been reported in this type of FIB-fabricated tungsten strips [18, 19]. These results, therefore, demonstrate a strong proximity induced superconductivity in GaN wall fragment from tungsten. R_{gn} and R_w vary quite differently with temperature around T_c for low values of B. While, R_w shows a monotonic reduction from its normal state value to zero at all fields, R_{gn} passes through a peak before dropping to zero at low fields. At higher fields $B > 0.5$ T, the peak is not observed.

Current flows through a S–Sm–S (or S–N–S) junction via two channels, the supercurrent (due to Andreev and Josephson processes) and the normal current associated with the transfer of quasi-particles (electrons) across the interfaces. Two Andreev reflections at the two S–N interfaces result effectively in transferring a Cooper pair from one superconducting lead to the other, if the electrons and holes are able to maintain phase coherence in the normal region. This channel naturally dominates for $T \ll T_c$. If the intervening space is an insulator the coherent transfer of the Cooper pairs is more likely to be a Josephson process. Flow of supercurrent through the GaN wall-fragments, where the superconducting contacts are separated by more than a micrometer, therefore, suggests that the phase coherence length l_ϕ of the carriers in the wall fragment must be of micrometer order.

Figures 3(a) and (b) compare the magnetic field ($B_{||}$) dependence of the wall fragment resistance $R_{gn}(B)$ (in device D1a) and the tungsten strip resistance $R_w(B)$ (in device D2), respectively, at different temperatures. At temperatures below 4.5 K, $R_w(B)$ shows a monotonic transition to zero from its normal state value when $B < B_c(T)$. On the other hand, $R_{gn}(B)$ passes through a broad peak before decreasing to zero with the reduction of B for temperatures below 4 K. For $T \geqslant 4$ K, $R_{gn}(B)$ goes through the peak but ends up at a non-zero value consistent with the $R(T)$ traces. (figure 2). A peak in the resistance near the superconducting transition, has been observed in the c-axis resistivity of layered high T_c superconductors and lamellar chalcogenides [20, 21] whose likely origin is the internal Josephson coupling between stacks of *ab* planes. This particular behaviour is however opposite to what is observed in layered compounds, where the peak in $R(T)$ gets stronger at higher B. We therefore look for a different possible explanation where the magnetic field must be suppressing a scattering mechanism. Superconducting contact to a ferromagnetic Co/Ni nanowire has been reported, showing a qualitatively similar feature as in figures 2(a) and 3(a) [22]. Although the origin of this feature is not fully understood, one might anticipate that the fluctuation of a magnetic moment in intervening area (either ferromagnetic or defect or surface related) would be suppressed once the applied magnetic field is strong enough. It thus appears that the peak in resistivity when the superconductivity just begins to set in, is consistent with the formation of a magnetic moment in the region between the contacts. Transport measurements on these GaN nanowall fragments with non-superconducting contacts as

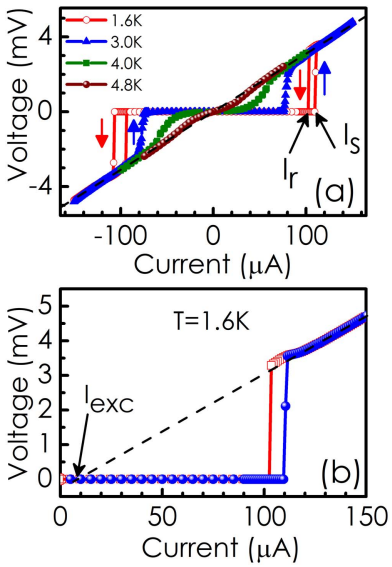

Figure 4. (a) *V–I* characteristic for device D1a recorded at different temperatures. (b) *V–I* characteristic for device D1a at 1.6 K depicting the excess current(I_{exc}). Here I_r denotes the retrapping current and I_c denotes the critical current of the junction.

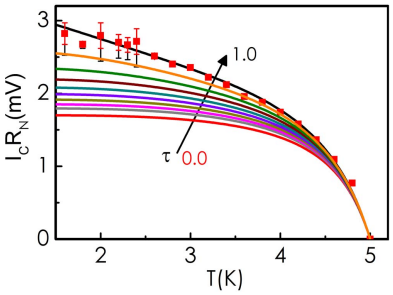

Figure 5. I_cR_N as a function of temperature. Solid red squares are the experimental data points. Dotted line represents the best fit profile using equation (1). The errors in the reported values of the fit parameters are about ~5%. $R^2 = 1 - \frac{\sum(y_i^{obs} - y_i^{fit})^2}{\sum(y_i^{obs} - \bar{y})^2}$ gives $R^2 = 0.95$, which is the 'goodness of fit'.

well as magnetic force microscopy imaging of these nanowalls suggest that a magnetic moment does develop at the surface of these polar wedges, even though there are no intentional ferromagnetic dopants. These data would be reported elsewhere.

Current–voltage (*I–V*) characteristics at different temperatures for devices D1a (figure 4) show a small but clear hysteresis at low temperatures. This can be attributed to the formation of a Josephson junction with small but non-zero shunt capacitance, which naturally arises due to the gap between the electrodes and oxide separating them from the conducting Si substrate. The observed critical current is $I_c(0) \approx 100\,\mu$A. We have verified (in device D2) that the critical current of the superconducting tungsten leads is $\approx 200\,\mu$A. The observed $I_c(T)$ in figure 4 can thus be attributed to the junction and not the leads themselves. We thus get the ratio of the Josephson coupling energy to thermal fluctuations, $\hbar I_c(0)/ek_BT_c \gg 1$. If the normal state part of the curve is extrapolated to $V = 0$ it cuts the current axis at a small but finite value. Existence of this 'excess current' is an indication of the flow of supercurrent through interfaces, with a weak barrier [23, 24]. For a Josephson Junction, I_{exc} approaches zero with increasing barrier strength, $Z = V_o/\hbar v_F$, where V_o the barrier height and v_F the Fermi velocity of the electrons. The data, therefore, suggests a small Z barrier at the S–Sm interface.

Product of the critical current at zero magnetic field and the normal state resistance (I_cR_N) for the device D1a is plotted as a function of temperature in figure 5. $I_cR_N(T)$ follows a convex-shaped curve, which is quite uncommon for a wide-junction [8]. Such a profile implies a ballistic flow of carriers through the normal conductor in a S–N–S junction [25, 26]. Decay profile of $I_c(T)$ with increasing temperature is typically concave-shaped or exponential for long-junctions, where the transport through the normal conductor is diffusive in nature.

The current–phase relation for a ballistic Josephson junction can be expressed as [27, 28]

$$I_s(\theta, \tau, T) = \frac{\pi\Delta(T)}{2eR_N} \frac{\sin\theta}{\sqrt{1 - \tau\sin^2\frac{\theta}{2}}} \times \tanh\left[\frac{\Delta(T)}{2k_BT}\sqrt{1 - \tau\sin^2\frac{\theta}{2}}\right], \quad (1)$$

where, τ is the transparency of the junction, and $\Delta(T) = \gamma k_BT_c \tanh(\gamma\sqrt{\frac{T_c}{T} - 1})$ describes the variation of superconducting gap with temperature [29]. The critical current is $I_c = \max(I_s)_\theta$. The best fit to the data gives $\gamma = 2.8$ and $\tau = 0.9$. γ is larger than the BCS value of 1.76. Also noticeable is the value of $\tau = 0.9$, very close to its ideal value of 1, suggesting highly transparent interfaces. This is again consistent with the finding of excess current I_{exc} in the wall fragment as shown in figure 4(b). These parameter values also confirm a ballistic transport of carriers over a distance of nearly 2 μm through the wall fragment. This can only arise when the scattering times are long enough to allow the proximity effect to engulf the entire normal region.

Finally, we note that the highest magnetic field at which we are still able to observe dissipationless transmission is clearly higher than 9 T, (figure 3) the highest magnetic field available in our experiments. This was already reached at $T \approx 1.6$ K and had not saturated. The $T = 0$ value is clearly going to be higher than the limit for the survival of a singlet Cooper pair, obtained by setting the Zeeman splitting of the single electron spin with the single particle gap i.e. $\mu_BB \approx 1.76k_BT_c$. A more refined calculation (the Clogston–Chandrasekhar limit [30, 31]) would give $B_c = 1.8\,T_c = 1.8 \times 4.5 = 8.1$ T, where the field is expressed in Tesla and the temperature in Kelvin. This observation may indicate formation of Cooper pairs with parallel spins (spin-triplet, with either non-chiral p_x or chiral $p_x + ip_y$). Experimentally SNS junctions where the normal metal has a helical magnetic structure have been prepared with aluminium and holmium [32] . Al is a conventional singlet superconductor and at low temperatures Ho supports a magnetic structure in which the

magnetization vector rotates along the c-axis at $T < 21$ K. In such structures singlet superconducting correlations are destroyed within a length scale of ferromagnetic coherence length of typically 1–10 nm, whereas the triplet correlations can persist for ~100 nm. Another case of $p_x + ip_y$ triplet pairing induced by proximity to a s-wave superconductor has been reported in junctions of a topological insulator Bi_2Se_3 and the singlet superconductor NbN [33]. In such junctions the differential conductance shows a form that is not possible to explain by assuming singlet Cooper pairs. A large body of theoretical work have addressed the possibility of triplet correlations in superconductor–ferromagnet structures in several geometries [34–37]. Even without a ferromagnet, a possible spin-accumulation has been theoretically predicted at the junction of a singlet and triplet superconductor [38, 39]. For $s - p_x$, $s - p_x + ip_y$ and $s - d_{x^2-y^2}$ junctions, calculations of the current–phase relations have been done by various authors. The current–phase relation, if different from the simple Josephson result ($I(\phi) \propto \sin\phi$) can lead to very different behaviour of the I–V relation for a single junction in zero or finite magnetic fields. Experimentally probing such junctions could clearly be one way of exploring triplet or more complex pairing in superconductors or conversion of a singlet current into triplet current at suitable interfaces.

In conclusion, we have demonstrated a proximity induced superconductivity and long coherence lengths in a combination of an unconventional 'dirty' superconductor and a wedge shaped polar semiconductor. The device, with ohmic contacts of high transparency, shows a remarkably robust superconducting state. The features observed in the I–V characteristics, show that the transport through a distance of almost 2 μm is nearly ballistic. However the critical temperatures and magnetic fields cannot be fully explained by assuming singlet Cooper pairs. In fact the critical field is clearly above the well known limit for singlet pairing [30, 31]. The devices were made with the several contacts (hence junctions) to the same piece of the semiconductor primarily for four-terminal measurements, making isolation of the properties of a single interface somewhat difficult to extract. These can however be made in different geometries where such properties are easier to extract. The presence of heavy nuclei like tungsten might lead to spin-orbit effects in the superconductor itself. The polar semiconductor (GaN) used here also has spin-orbit effects, although it is not as strong as in the case of some other III–V materials like InAs, for example.

Acknowledgments

We acknowledge support from Department of Science and Technology, Government of India under project: SR/S2/CMP-71/2012, DST-FIST and central facilities of IIT Bombay. We also thank B Pal, A Jain and B P Joshi for experimental assistance. We thank Marius Bienek, Dr Christoph Somsen and Dr Gunther Eggeler for technical assistance and for the use of their FIB.

ORCID iDs

Swarup Deb https://orcid.org/0000-0002-2919-0608
Andreas Wieck https://orcid.org/0000-0001-9776-2922
K Das Gupta https://orcid.org/0000-0002-3941-0520

References

[1] Alicea J, Oreg Y, Refael G, Von Oppen F and Fisher M P 2011 *Nat. Phys.* **7** 412
[2] Gangadharaiah S, Braunecker B, Simon P and Loss D 2011 *Phys. Rev. Lett.* **107** 036801
[3] Weinstock H and Ralston R W 2012 *The New Superconducting Electronics* (*Nato Science Series E, Applied Sciences* vol 251) (Dordrecht: Kluwer)
[4] Clarke J and Wilhelm F K 2008 *Nature* **453** 1031
[5] Holm R and Meissner W 1933 *Z. Phys.* A **86** 787
[6] Wan Z, Kazakov A, Manfra M J, Pfeiffer L N, West K W and Rokhinson L P 2015 *Nat. Commun.* **6** 7426
[7] Nitta J, Akazaki T, Takayanagi H and Arai K 1992 *Phys. Rev.* B **46** 14286
[8] Lee G-H, Kim S, Jhi S-H and Lee H-J 2015 *Nat. Commun.* **6** 6181
[9] Doh Y-J, van Dam J, Roest A L, Bakkers E P A M, Kouwenhoven L P and Franchesi S D 2005 *Science* **309** 272
[10] Deb S, Bhasker H, Thakur V, Shivaprasad S and Dhar S 2016 *Sci. Rep.* **6** 26429
[11] Kesaria M and Shivaprasad S 2011 *Appl. Phys. Lett.* **99** 143105
[12] Zhong A and Hane K 2012 *Nanoscale Res. Lett.* **7** 686
[13] Zhong A and Hane K 2013 *Japan. J. Appl. Phys.* **52** 08JE13
[14] Zhong A, Sasaki T and Hane K 2014 *Int. J. Hydrog. Energy* **39** 8564
[15] Bhasker H, Dhar S, Sain A, Kesaria M and Shivaprasad S 2012 *Appl. Phys. Lett.* **101** 132109
[16] Bhasker H, Thakur V, Shivaprasad S and Dhar S 2015 *J. Phys. D: Appl. Phys.* **48** 255302
[17] Bhasker H, Ghosh P, Ghosh A, Mukherjee A, Singh B and Dhar S 2012 *AIP Conf. Proc.* **1447-1** 1089–90
[18] Li W, Fenton J, Wang Y, McComb D and Warburton P 2008 *J. Appl. Phys.* **104** 093913
[19] Sun Y, Wang J, Zhao W, Tian M, Singh M and Chan M H 2013 *Sci. Rep.* **3** 2307
[20] Szabó P, Samuely P, Kačmarčík J, Jansen A, Briggs A, Lafond A and Meerschaut A 2001 *Phys. Rev. Lett.* **86** 5990
[21] Gray K and Kim D 1993 *Phys. Rev. Lett.* **70** 1693
[22] Wang J, Singh M, Tian M, Kumar N, Liu B, Shi C, Jain J, Samarth N, Mallouk T E and Chan M H 2010 *Nat. Phys.* **6** 389
[23] Blonder G, Tinkham M and Klapwijk T 1982 *Phys. Rev.* B **25** 4515
[24] Giazotto F, Grove-Rasmussen K, Fazio R, Beltram F, Linfield E and Ritchie D 2004 *J. Supercond.* **17** 317
[25] Likharev K 1979 *Rev. Mod. Phys.* **51** 101
[26] Kulik I and Omel'Yanchuk A 1977 *Sov. J. Low Temp. Phys.* **3** 945
[27] Haberkorn W, Knauer H and Richter J 1978 *Phys. Status Solidi* a **47** K161–4
[28] Bagwell P F 1992 *Phys. Rev.* B **46** 12573
[29] Senapati K, Blamire M G and Barber Z H 2011 *Nat. Mater.* **10** 849
[30] Clogston A M 1962 *Phys. Rev. Lett.* **9** 266
[31] Chandrasekhar B 1962 *Appl. Phys. Lett.* **1** 7
[32] Sosnin I, Cho H, Petrashov V T and Volkov A F 2006 *Phys. Rev. Lett.* **96** 157002

[33] Koren G, Kirzner T, Kalcheim Y and Millo O 2013 *Eur. Phys. Lett.* **103** 67010
[34] Alidoust M, Halterman K and Valls O T 2015 *Phys. Rev.* B **92** 014508
[35] Alidoust M and Halterman K 2015 *New J. Phys.* **17** 033001
[36] Alidoust M and Halterman K 2015 *J. Appl. Phys.* **117** 123906
[37] Alidoust M and Halterman K 2015 *J. Phys.: Condens. Matter* **27** 235301
[38] Sengupta K and Yakovenko V M 2008 *Phys. Rev. Lett.* **101** 187003
[39] Tanaka Y 1994 *Phys. Rev. Lett.* **72** 3871